Plasma Science and Technology

PAPER

Controlling fine particles in flue gas from lead-zinc smelting by plasma technology

Plasma Sci. Technol. **22** (2020) 044004 (9pp) https://doi.org/10.1088/2058-6272/ab77d3

Controlling fine particles in flue gas from lead-zinc smelting by plasma technology

Tao ZHU (竹涛)[1,2,3], **Ruonan WANG** (王若男)[1,2], **Xing ZHANG** (张星)[1,2], **Yiwei HAN** (韩一伟)[1,2], **Wenfeng NIU** (牛文凤)[1,2], **Zeyu XUE** (薛泽宇)[1,2] and **Lifeng WANG** (王礼锋)[1,2]

[1] Institute of Atmospheric Environmental Management and Pollution Control, China University of Mining & Technology (Beijing), Beijing 100083, People's Republic of China
[2] State Key Laboratory of Organic Geochemistry, Guangzhou Institute of Geochemistry, Chinese Academy of Sciences, Guangzhou 510640, People's Republic of China
[3] Shaanxi Key Laboratory of Lacustrine Shale Gas Accumulation and Exploitation (under planning), Shaanxi Province 710065, People's Republic of China

E-mail: bamboozt@cumtb.edu.cn

Received 2 September 2019, revised 17 February 2020
Accepted for publication 19 February 2020
Published 17 March 2020

Abstract

With the aim of controlling the problem of fine particles in the flue gas of lead-zinc smelting, a low-temperature plasma-electrocoagulation and electric bag composite dedusting experimental platform was designed by combining electrocoagulation and electric bag composite dust removal technology based on the research of low-temperature plasma technology. Firstly, the properties of fine particles in flue gas from lead-zinc smelting were analyzed, and the effects of input voltage, filter wind speed, dust concentration, and pulse-jet ash-cleaning cycle on the dust collection efficiency of the integrated device were studied. Then, the energy efficiency of the integrated technology was analyzed, and the control mechanism of the fine particles was revealed. The experimental results show that the integrated technology of low-temperature plasma-electrocoagulation and electric bag composite dust removal achieves a fine particle removal efficiency of more than 99.99% and the energy consumption per unit mass of the dust is only 0.008 kW · h/g. The integrated technology has broad application prospects and far-reaching practical significance for the lead-zinc smelting industry to achieve ultra-low emission targets for flue gas and achieve energy-saving and emission reduction effects.

Keywords: lead-zinc smelting smoke, fine particles, low-temperature plasma, low-temperature plasma-electrocoagulation and electric bag compound dust removal integrated technology

(Some figures may appear in colour only in the online journal)

1. Introduction

At present, China's atmospheric environmental quality presents the characteristics of a high pollution load and multi-pollutant superposition, and the pollution type gradually changes from the traditional coal smoke type to the composite type with PM2.5 (particulate matter smaller than 2.5 micrometers) and O_3 as the main pollutants [1–3]. Fine particles in lead-zinc smelting smoke has a large specific surface area, and heavy metals (Pb, Hg, As, Cd) are easily accumulated, high in content, and highly toxic, and contribute to PM2.5 emissions, polluting the regional atmospheric environment and harming human health. Therefore, effective control of fine particles in lead-zinc smelting smoke is urgently needed [4–6].

Currently, filter bags, static electricity precipitators, and other traditional dust removal technologies are widely used in the lead-zinc smelting industry. Although the overall dust removal efficiency is more than 99%, the removal efficiency of fine particles is low, which makes it impossible to effectively control fine particles in lead-zinc smelting smoke [7–11]. The emergence of electrocoagulation provides a new perspective for solving the fine particles pollution control problem: by free charge and discharge of the collision to

Table 1. Qingdao Laoying 3012-08 smoke test parameters.

Main parameters	Sampling flow ($l\,min^{-1}$)	Flue gas dynamic pressure (Pa)	Flue gas static pressure (kPa)	Pressure in front of the flowmeter (kPa)	Temperature in front of the flowmeter (°C)	Flue gas temperature (°C)
Range of parameters	5–80	0–2000	–30–30	–30–0	–30–150	0–500
Resolution	0.1	1	0.01	0.01	0.1	1
Accuracy rate	±2.5%	±2.0%	±4.0%	±2.5%	±1.5%	±3.0%

improve the ability of fine particulate matter charge, enhancing the coalescence effect between the dust particles that formed fine particles coagulate, and re-union size larger coarse particulate matter, and then through traditional dust removal, thereby improving fine particle removal efficiency [12–18]. Electrocoagulation technology has been gradually applied to dust removal in coal-fired power plants, cement kilns, and other dust removal applications. In this paper, a low-temperature plasma-electrocoagulation and electric bag composite dedusting experimental platform was designed by combining electrocoagulation and electric bag composite dust removal technology based on the research of low-temperature plasma technology. Firstly, fine particles were charged and combined into coarse particles by a low-temperature plasma-electric coagulation device, and then the fine particles in the lead-zinc smelting flue gas were collected by an electric bag composite precipitator.

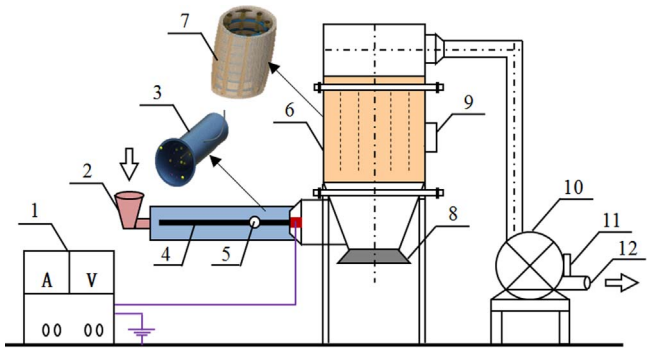

Figure 1. Low-temperature plasma-electrocoagulation and electric bag composite dust removal experimental platform. 1—power box, 2—dust generator, 3—low-temperature plasma-electric coagulation unit, 4—corona wire, 5—observation hole, 6—electrostatic and fabric composite filter, 7—electric cage bag, 8—dust hopper, 9—control panel, 10—fan, 11—airflow adjusting valve, 12—air outlet.

2. Experimental system and method

2.1. Experimental system

This experimental system is composed of two parts: the sampling and detecting device, low-temperature plasma-electrocoagulation, and the electric bag composite dust removal integrated experimental platform. The sampling and detecting device includes an Anderson particle impact sampler and a Qingdao Laoying 3012-08 smoke tester.

The Anderson particle sampler is designed based on the principle of aerodynamics, in which different particle sizes of dust are separated and collected at different levels in sampling filter membranes, and a unit density ($1\,g\,cm^{-3}$) spherical particle is used for calibration. All the collected dust particles, regardless of their density, volume, and shape differences, were graded according to the aero-dynamic particle size equivalent to the reference particle, and the mass of each dust particle was obtained by weighing the sampling filter film at each level, thus the mass parameters were calculated [19].

The Qingdao Laoying 3012-08 smoke test instrument is designed based on the principle of pitot tube constant speed sampling. During the sampling process, the sampling nozzle was placed at the detection point and a certain amount of dust was extracted in the direction of the airflow. The concentration and total emission of the particulate matter could be calculated by recording the smoke and dust quality collected by the filter and the volume of the extracted gas. The instrument parameters are shown in table 1 [20].

The integrated experimental platform of low-temperature plasma-electrocoagulation combined with electric bag dust removal is shown in figure 1. It adopts a high-voltage direct current (DC), with an input voltage of 220 V and a rated output voltage of 50 kV. The structure of the low-temperature plasma-electric coagulation device is of the wire-tube type, the length of the tube is 700 mm, the diameter is 200 mm, the wall of the tube is the grounding pole, the center line of the tube is the corona line, the diameter is 1 mm and is connected to a high-voltage power supply, and the material is stainless steel, corrosion resistant, and low priced. The electric bag composite filter consisted of 12 glass fiber coated filter bags sized $\phi 180 \times 1500$ mm, with a layout format of 3×4, and the ash removal method used was pulse back blowing. During the experiment, voltage was applied to the cage bone supporting the filter material, and an electrostatic field was applied to polarize the surface of the filter material, strengthen the collection of the charged dust particles by the filter material, reduce the impact of the filter wind speed and dust particles on the filter material, and prevent dust particles from penetrating into the fiber root [21]. The specific parameters of the cloth bag are shown in table 2.

In the experimental study, the dust generator was used to simulate the flue gas of lead and zinc smelting. The dust of each particle size section is proportioned and mixed evenly. The dust generating device is modified from an electric feeder. The fan speed is adjusted to generate different air volume, and the maximum air volume is $800\,m^3\,h^{-1}$. The basic parameters of the equipment running under an empty load are shown in table 3, where the formula for calculating

Table 2. The parameters of the designed bag filter.

Material	Gram weight ($g\,m^{-2}$)	Thickness (mm)	Radial tension ($N/5 \times 20$ cm)	Latitudinal tension ($N/5 \times 20$ cm)	Ventilation property ($m^3\,m^{-2}$·min)	Adaptive temperature (°C)
Fiber glass	900	1.75	>1800	>1800	8–15	260–300

Table 3. The elemental operational parameters of the designed unit without load.

Gas flow ($m^3\,h^{-1}$)	Plasma-electric coagulation device airflow velocity ($m\,s^{-1}$)	Plasma-electric coagulation device residence time (s)	Electrostatic fabric composite filter wind speed ($m\,min^{-1}$)	Overall pressure loss (Pa)
800	7.08	0.10	1.27	570
698	6.17	0.11	1.11	450
580	5.13	0.14	0.92	360
502	4.44	0.16	0.80	280
395	3.54	0.20	0.63	200

the filtration wind speed is

$$V_{\mathrm{F}} = \frac{q_v}{60A} \tag{1}$$

$$A = n \times \left(\pi dl + \pi\frac{d^2}{4}\right), \tag{2}$$

where V_{F} is the filtered wind speed, $m\,min^{-1}$. q_{v} is the flue gas flow rate, $m^3\,h^{-1}$. A is the total filtration area of the electrostatic enhanced bag filter, m^2; d is the diameter of the filter bag, m, and d is 0.18 m; l is the length of the filter bag, m, and l is 1.5 m; n is the number of the filter bag, and n is 12.

3. Results and discussion

In this study, the characteristics of fine particulate matter in lead-zinc smelting flue gas were analyzed, and the effects of input voltage, filtration wind speed, dust concentration, and pulse dust blowing period on the dust removal efficiency of the integrated unit were studied. For the fine particulate matter, PM3.3 is selected to consider the best operating condition to analyze the energy efficiency of the integrated technology and reveal its control mechanism for fine particulate matter.

3.1. Analysis of the fine particle properties

The dust used in the experiment was taken from the bag filter of the blast furnace of the Shaoguan smelting plant and its particle size was less than 100 μm. The specific surface area of the dust was about 8.297 76 $m^2\,g^{-1}$, and the content of PM3.3 was 7.5%. The specific resistance of the fine particulate matter in the lead-zinc smelting flue gas was tested by means of a DR-3 type high-pressure dust specific resistance tester. The test voltage was 4.0 kV, and the specific resistance changed with temperature, as shown in figure 2. It increased with the rise in temperature, and when the temperature was 120 °C it peaked at $2.78 \times 10^{12}\ \Omega \cdot$ cm, then decreased gradually with the rise in temperature. The order of magnitude of the dust specific resistance was maintained at $10^{12}\ \Omega \cdot$ cm.

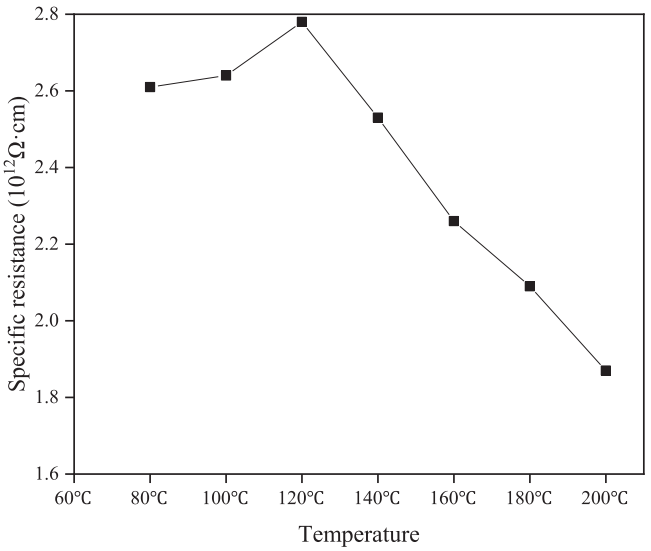

Figure 2. Specific resistance.

Through a large number of studies, Yuan and Pan showed that the dust specific resistance measured by the DR-3 type high-pressure dust specific resistance tester was 1−3 orders of magnitude higher than the actual specific resistance of the working condition [22]. In this experimental study, the specific resistance of the lead and zinc smelting gas fine particulate matter in the corresponding working condition was in the range of 10^9–$10^{11}\ \Omega \cdot$ cm. Therefore, dust can be charged and treated by electrocoagulation.

3.2. Influence of input voltage

For the low-temperature plasma-electric coagulation device, when the DC high pressure was applied to the discharge electrode, a strong corona discharge area would appear in a very small area around the discharge electrode, producing a large number of high-energy free electrons, and the gas molecules would be highly ionized, resulting in the existence of both high-energy free electrons and positive and negative gas ions in this area.

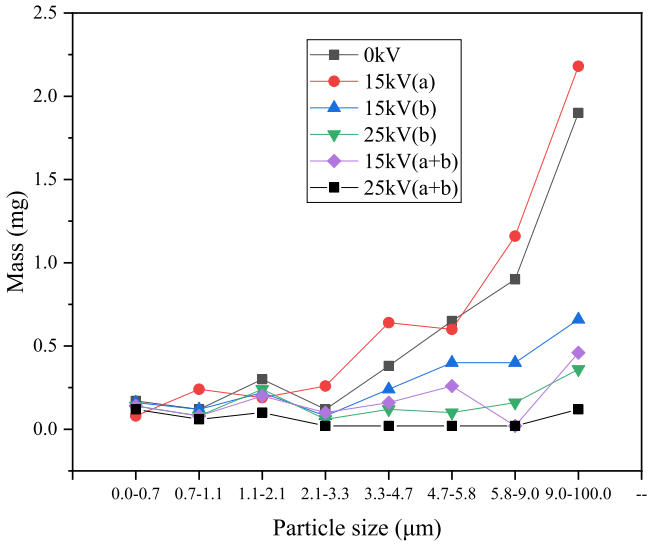

Figure 3. Distribution of the sizes of the particle emissions.

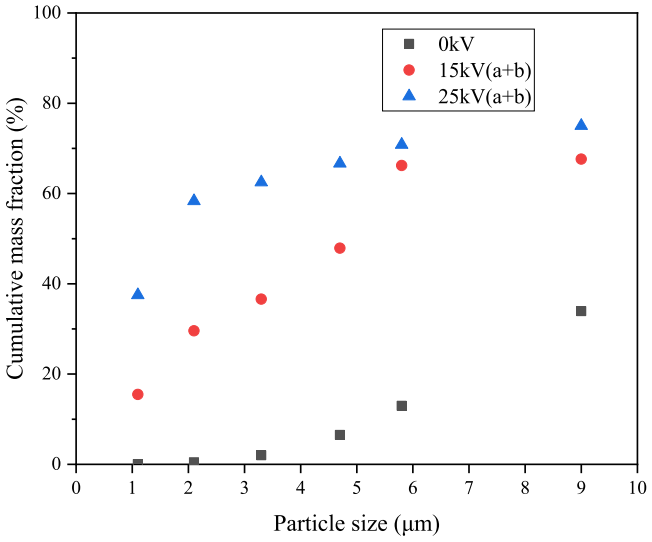

Figure 4. Cumulative mass fraction of the particle emission size distribution.

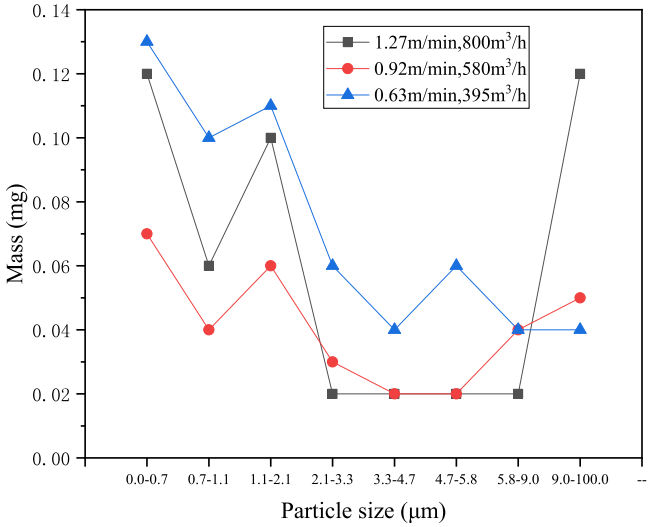

Figure 5. Distribution of the velocity/volume of the filter.

In the negative DC corona discharge, the wire electrode is connected to the negative DC high-voltage power supply. The corona discharge area is only limited around the online electrode. Only the negative ions and free electrons in the plasma generated by the corona discharge move toward the anode under the action of an electric field force. Free electrons outside the corona region, due to a sharp reduction in energy, attach themselves to the gas molecules to form a large number of negative ions. The positive ions move toward the cathode. In the negative DC electric field, most of the fine particles collide with negative ions and are charged, while only a few can collide with positive ions near the cathode. Therefore, the comprehensive charged effect of the particles is a negative charge [23].

When voltage is applied to the cage bone of the electric bag composite precipitator, the condensation of fine particles in the lead and zinc smelting smoke increases, while the glass fiber of the filter bag is negatively charged. When fine particles are deposited on the surface of the filter bag, due to a certain electrostatic effect, the dust layer is loose, the clearance between the fiber and the dust layer is suitable, and cleaning the dust is easy. The porosity between individual fibers increases, and the pressure loss decreases at a slower rate. At the same time, the fiber oscillates due to the effect of the flow field, which increases the collision between the fiber and the particle, and enhances the interception effect and electrostatic effect [24].

Figure 3 shows the particle size distribution of the smoke that escaped at the air outlet under different voltage conditions. In order to comprehensively analyze the influence of input voltage on the dust removal efficiency of the integrated device, voltages were applied to the low-temperature plasma-electric coagulation unit and electric bag composite dust collector, respectively. For the convenience of expression, the above two parts are abbreviated as a and b, and the applied voltages are 0, 15 (a), 25 (a), 15 (b), 25 (b), 15 (a + b), and 25 kV (a + b), respectively. In the experiment, the smoke inlet concentration was set to be 6.0 g m^{-3}, the filter wind speed was 1.27 m min^{-1}, the fixed monitoring time was 240 min, the ash-removal cycle T was 40 min, the pulse injection pressure was stable at 0.2–0.4 MPa, the frequency was 0.5 Hz, and the ash removal time was about 3 min within one cycle.

It can be seen from figure 4 that under different voltage conditions, the removal effects of fine particles ranges from high to low in general, which are 25 (a + b), 15 (a + b), 25 (b), 25 (a), 15 (b), 0, and 15 kV (a). The effect of dust collection using the electric bag composite dust collector is higher than that using the low-temperature plasma-electric coagulation device, but it is not as good as the combined effect of the two.

Figure 4 shows the mass fraction of the smoke that escaped at the outlet of the integrated device under different voltage conditions. As can be seen from figure 5, the mass fraction of the escaping soot changes after the flue gas passes

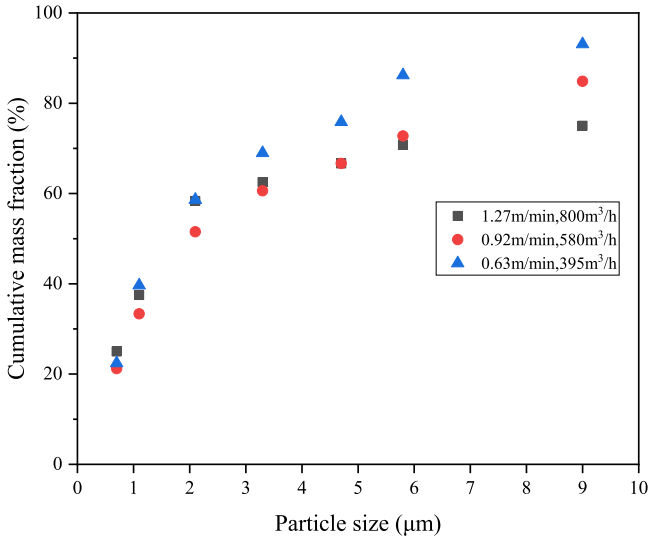

Figure 6. Cumulative mass fraction of the velocity/volume of the filter.

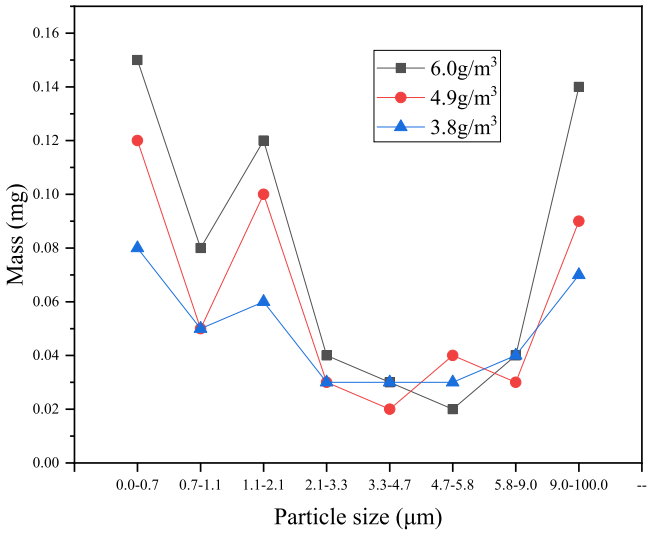

Figure 7. Distribution of the concentration of the fume particulate.

through the integrated dust removal device. Under the conditions of 15 and 25 kV, the mass fraction of PM3.3 increased from 2% to 36.6% and 62.5%, respectively. With the increase of voltage, the efficiency of collecting the fine particles gradually increased.

3.3. Influence of filter velocity and volume

Figure 5 shows the particle size distribution of the smoke that escaped at the outlet under different filtration wind speed conditions, and figure 6 shows the mass fraction under the corresponding conditions. In the experiment, the filtration wind speed was set to be 1.27, 0.92, and 0.63 m min^{-1} respectively, and the corresponding air volume was successively 800, 580, and 395 m^3 h^{-1}. The smoke inlet concentration was 6.0 g m^{-3}, the fixed monitoring time was 240 min, the dust cleaning cycle T was 40 min, the filtration wind speed was 1.27 m min^{-1}, the pulse injection pressure was stable at 0.2−0.4 MPa, the frequency was 0.5 Hz, the dust cleaning time was about 3 min, and a 25 kV (a + b) voltage was applied.

As can be seen from figures 5 and 6, under different filtering wind speeds, the removal effects of fine particles were 0.92, 1.27, and 0.63 m min^{-1} from high to low, respectively. The escape rate of the fine particulate is high, and the mass percentage of the fine particulate with a particle size less than 3.3 μm reaches above 60%. The reason is that the filter wind speed is too high, the dust particles stay in the low-temperature plasma-electrocoagulation device for a short time, the charged electrocoagulation is not sufficient, and the electric bag composite precipitator cannot effectively capture the fine particles, resulting in a high escape rate of fine particles. Therefore, filter wind speed should be reasonably configured according to the actual treatment requirements to improve the removal efficiency of the fine particulate matter.

There are both positive and negative charges on the fiber surface, but in the initial stage, there are few particles filtered to the fiber surface, and there are enough negative charges on the fiber surface to interact with positively charged particles. Therefore, only the attraction of opposite charges is considered here, and the Coulomb forces of the same kind of repulsion are not considered. The dimensionless number (N_c) determining the Coulomb force is [25]:

$$N_c = \frac{C\sigma ne}{3\pi\mu(1+\varepsilon)V\varepsilon_0 d_p}, \tag{3}$$

where C is the Cunningham slip correction factor, σ is the charge density of the fiber, μ is the viscosity of the fluid, n is the charge of the particle, e is the unit charge, 1.6×10^{-19} C, ε is the dielectric constant of the fiber, ε_0 is the dielectric constant for a vacuum, d_p is the particle diameter, and V is the velocity of the fluid. From the formula (3), we can see that the dimensionless number (N_c) of the Coulomb force is inversely proportional to the first power of the particle size (d_p) and the first square of the fluid velocity (V). In other words, the smaller the diameter of the particles, the slower the flow rate, the greater the Coulomb force, the stronger the mutual attraction, and the more obvious the improvement in the initial filtration efficiency is. On the contrary, the larger the diameter of the particles is, the smaller the Coulomb force will be, the weaker the mutual attraction will be, and the improvement of the initial filtration efficiency will be less obvious.

3.4. Influence of dust concentration

Figure 7 shows the particle size distribution of the smoke that escaped at the air outlet under different smoke concentration conditions, and figure 8 shows the dust collection efficiency under the corresponding conditions. In the experiment, the concentrations of the dust inlet were set as 3.8, 4.9, and 6.0 g m^{-3} respectively, the air volume was 800 m^3 h^{-1}, the fixed monitoring time was 240 min, the ash-cleaning cycle was 40 min, the filter wind speed was 1.27 m min^{-1}, the pulse injection pressure was stable at 0.2–0.4 MPa, the frequency

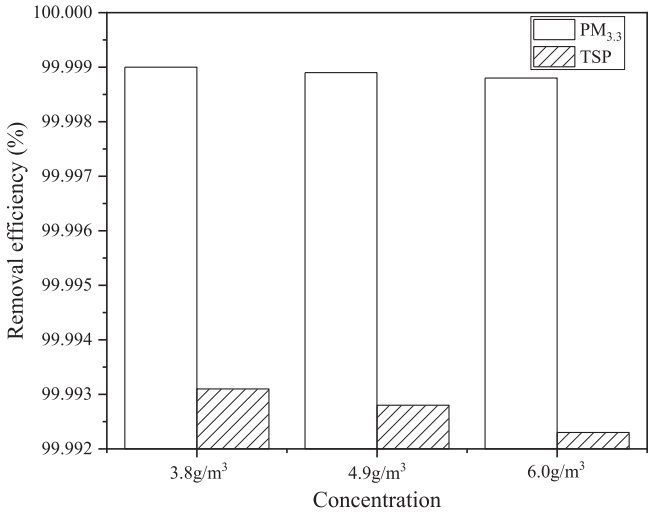

Figure 8. Removal efficiency of fume particles with different concentrations.

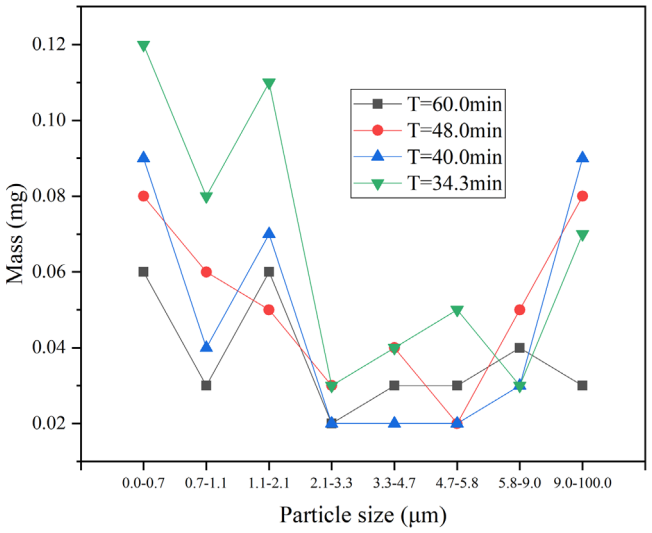

Figure 10. Distribution of the different ash-cleaning cycle.

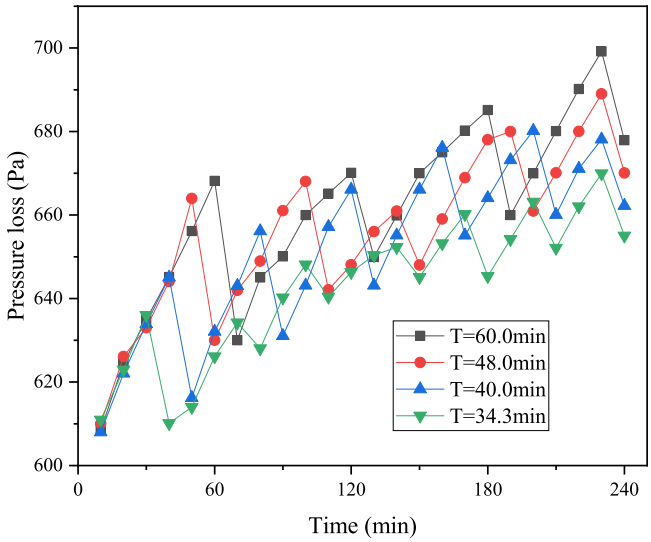

Figure 9. Distribution of the pressure losses of dust particles cleared under different periodic cycles.

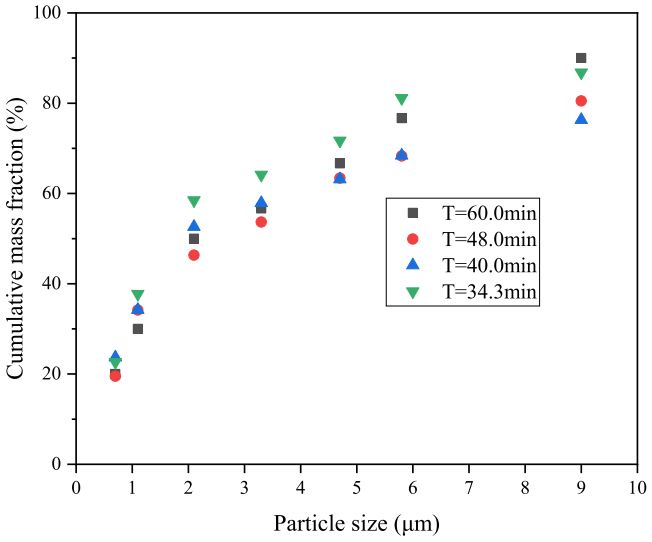

Figure 11. Cumulative mass fraction of the different ash-cleaning cycle.

was 0.5 Hz, the ash-cleaning time was about 3 min within a cycle, and a 25 kV (a + b) voltage was applied.

It can be seen from figures 7 and 8 that under different smoke concentration conditions, all of the fine particles appear escape peak at the particle size range of 1.1–2.1 μm. For the total suspended particulates (TSPs) and PM3.3, the removal efficiency of fine the particulate matter was more than 99.99%. Under different dust concentration conditions, the removal efficiency of PM3.3 is 6.0, 4.9, and 3.8 g m^{-3} from high to low, respectively. However, the removal efficiency is not different, indicating that the integrated device is suitable for lead and zinc smelting flue gas with different smoke concentrations.

3.5. Influence of the pulse-jet ash-cleaning cycle

Figure 9 shows the pressure losses under the conditions of different pulsed-jet ash-removal cycles, and figures 10 and 11 show the particle size distribution and mass fraction of the dust that escaped at the air outlet under the corresponding conditions. In the experiment, the concentration of the dust inlet was set as 6.0 g m^{-3}, the fixed monitoring time was 240 min, the ash-cleaning cycles T were 60, 48, 40, and 34.3 min, respectively, spraying was performed 4, 5, 6, and 7 times, the filter wind speed was 1.27 m min^{-1}, the pressure loss was recorded every 10 min, the pulse injection pressure was stable at 0.2–0.4 MPa, the frequency was 0.5 Hz, the ash-cleaning time was about 3 min within a cycle, and a 25 kV (a + b) voltage was applied.

As can be seen from figures 9–11, the pressure losses of the electric bag composite filter from high to low are 60, 48, 40, and 34.3 min, respectively, under the conditions of different pulse-jet ash-cleaning cycles. When the cleaning cycle increases, the dust particles attached to the filter bag increase, and the filtration resistance increases, so the pressure loss is

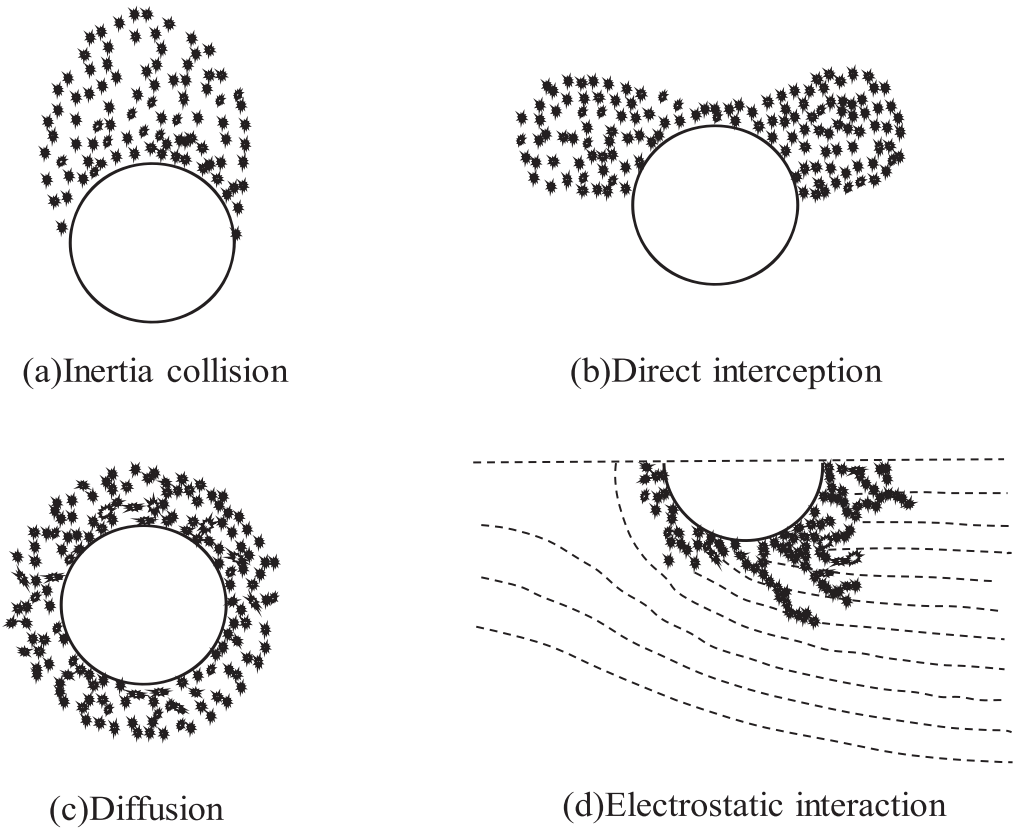

Figure 12. Particle chain shapes under different filtration mechanisms.

Table 4. Analysis of the dust removal efficiency of the integrated device.

	Dust		PM3.3	
Working condition	Exit concentration (μg m^{-3})	Efficiency (%)	Exit concentration (μg m^{-3})	Efficiency (%)
0 kV	357.3	99.9937	56.9	99.9874
25 kV (a + b)	47.1	99.9992	29.4	99.9935

higher under the same condition of ash removal cycle. The reason is that when the soot deposition on the surface of the cage bone of the cloth bag reaches a certain thickness, the attached dust particles and the falling dust particles maintain a state of equilibrium, and the pressure loss gradually tends stabilize. For fine particles whose particle size is less than 3.3 μm, the escape rate with a cleaning cycle of 34.3 min is significantly higher than that of the other three, and the overall dust removal efficiency is poor. The reason is that frequent dust removal destroys the gap of the cloth bag's glass fiber with dust particles, thus reducing the collection efficiency of fine particles.

When particles are trapped by fibers, they form dendritic chains on the fibers. The shape of the particle chain varies with the filtration mechanism of the particles. Figure 12 shows the particle chain shapes formed under different filtration mechanisms [26].

For the polydisperse particles used in this study, the dominant filtration mechanism is direct interception and the electrostatic effect. As can be seen from figure 12, both mechanisms can easily form long chains of particles. This kind of particle chain is not very stable, which can form continuously on the fiber, but is also prone to collapse under the action of external forces. The formation and collapse of the particle chain occur simultaneously in the process of dust collection, which may lead to the difference in the filtration resistance rising curve and dust capacity under different particle concentrations.

3.6. Analysis of energy efficiency

According to the above research, the operating conditions with a high dust removal efficiency of the integrated device are selected. The dust inlet concentration is 6.0 g m^{-3}, the initial air volume is 800 m^3 h^{-1}, the ash removal cycle T is 40 min, the filter's wind speed is 1.27 m min^{-1}, and the dust removal efficiency is stable and good when a 25 kV (a + b) voltage is applied. Under this working condition, the escape efficiency parameters of the soot outlet are shown in table 4. It

can be seen that the dust capture efficiency increases from 99.9937%–99.9992%, and the emission reduction reaches 310.2 g m^{-3}. For PM3.3, the capture efficiency was increased from 99.9874%–99.9935%, and the reduced displacement reached 27.5 g m^{-3}.

The specific energy consumption of the integrated low-temperature plasma-electric coagulation and electric bag composite dust removal device is as follows: the energy consumption of a 25 kV (a + b) voltage is 2 W, the energy consumption of online monitoring is 50 W, the energy consumption of the pulse-jet ash removal is 20 W, the energy consumption of the fan is 2200 W, and the overall power is 2272 W. The specific costs are as follows: when the inlet concentration of the dust is 6.0 g m^{-3}, the emission reduction is 310.2 g m^{-3}, the energy consumption per unit of emission reduction quality is 0.008 kW · h g^{-1}, and the unit's electric consumption is 0.8 CNY/kW · h, so the emission reduction cost per unit of lead and zinc smelting smoke and dust is 6.4 CNY/kg.

4. Conclusions

In this paper, a low-temperature plasma-electrocoagulation and integrated dedusting device with an electric bag was used to study the control of fine particles in lead-zinc smelting flue gas, and the following main conclusions were drawn:

(1) In the low-temperature plasma device, the charge and coagulation of fine particles were carried out in the same area, so as to enhance the charge capacity of the fine particles and the effect of interparticle coalescence, promote the effective collision of fine particles, improve the efficiency of the electric field charge and diffusion charge, and aggregate fine particles to form coarse particles. In this stage, the filter wind speed should be reasonably allocated according to the actual working conditions and treatment requirements to avoid the decrease of fine particle collection efficiency caused by inadequately charged coagulation.

(2) In the electric bag composite dust remover, the charged dust particles first settle in the glass fiber layer. When it reaches a certain degree, the charged dust particles form a dust layer on the fiber surface, and then the surface of the filter material is polarized by the electrostatic field. Due to the action of the flow field, the swing of the filter material fiber produces a brush effect, which strengthens the collection of charged dust particles by the filter material.

(3) Under different filtration wind speeds, the removal efficiency of fine particles by low-temperature plasma and electrocoagulation combined with electric bag dedusting technology was 0.92, 1.27, and 0.63 m min^{-1}, respectively. The longer the cleaning cycle of the integrated device is, the greater the pressure loss will be. Even under the same cleaning cycle, the pressure loss will gradually increase first, and the increase will slowly decrease until a state of equilibrium is finally reached. When the period of ash removal is short, although the pressure loss is small, the effect of fine particle collection is poor.

(4) Under different voltage conditions, the dedusting efficiency of the integrated device is in order from high to low as follows: 25 (a + b), 15 (a + b), 25 (b), 25 and 15 (a) (b), 0 and 15 kV (a). Neither the low-temperature plasma-electrocoagulation device nor the electrobag composite dust collector can effectively remove fine particles. The integrated technology considers the excellent dust removal characteristics of the above two parts. The removal efficiency of fine particles can reach 99.99% and the energy consumption per mass unit of dust is only 0.008 kW · h/g.

Acknowledgments

This work is supported by the State Key Laboratory of Organic Geochemistry, GIGCAS (No. SKLOG-201909) and the Fundamental Research Funds for the Central Universities (2009QH03). This research was funded by the Open Foundation of Shaanxi Key Laboratory of Lacustrine Shale Gas Accumulation and Exploitation (under planning).

References

[1] Gan L and Hu X S 2016 *Environ. Sci. Pollut. Res.* **23** 8470
[2] Oesch S and Faller M 1997 *Corros. Sci.* **39** 1505
[3] Li K F 2016 Researches on the cause of and the governance policy to urban air pollution in China *MSc Thesis* Southwestern University of Finance and Economics (in Chinese)
[4] Wang F *et al* 2016 *Nonferrous Metals Eng.* **6** 96 (in Chinese)
[5] Zhou D *et al* 2016 *Powder Technol.* **289** 52
[6] Cao R J *et al* 2017 *J. Cleaner Prod.* **161** 1459
[7] Yan K P *et al* 2017 *High Voltage Eng.* **43** 476 (in Chinese)
[8] Li Z H *et al* 2013 *J. Dalian Univ. Technol.* **53** 435 (in Chinese)
[9] Song Y C and Xu Y M 2015 *Metall. Equip.* 77 (in Chinese)
[10] Zhu J B *et al* 2010 *J. Electrostat.* **68** 174
[11] Gitterman H 2015 *J. Soc. Motion Pict. Eng.* **39** 70
[12] Zhu T *et al* 2015 *Clean Coal Technol.* **21** 6 (in Chinese)
[13] Zhang X, Lin H J and Hu B 2018 *Sep. Purif. Technol.* **200** 112
[14] Kamarehie B *et al* 2018 *Data Brief* **18** 96
[15] Zhao L 2013 Research on simultaneous removal of $PM_{2.5}$ and NO_x from flue gas by pulsed corona discharge *PhD Thesis* Zhejiang University (in Chinese)
[16] Khandegar V and Saroha A K 2012 *Chin. J. Chem. Eng.* **20** 439
[17] Munkhbayar B *et al* 2013 *Composites* B **54** 383
[18] Zou Z L *et al* 2017 *J. Electrostat.* **88** 106
[19] Tian Z X 2017 Study on the determination and analysis of single particle properties of atmospheric coarse particles—take Cologne (Germany) and Beijing (China) as examples *PhD Thesis* China University of Geosciences (Beijing) (in Chinese)
[20] Zhang Y S *et al* 2014 *Chin. Environ. Sci.* **34** 2741
[21] Zhang X X 2014 Explore on the mechanism of technology for the high-efficiently collection of fine particles by electrostatic-fabric precipitator *MSc Thesis* North China Electric Power University, Beijing, China (in Chinese) (https://doi.org/10.7666/d.D759350)

[22] Yuan Y T and Pan X L 2013 *Proc. 15th Conf. of ESP* 435
[23] Jiang J P 2015 Research on particle charging mechanism and coagulation removal of $PM_{2.5}$ by pulsed corona discharge *PhD Thesis* Zhejiang University (in Chinese)
[24] Liu Z B 2011 Theoretical and experimental research on the particles capturing of electric-bag hybrid *MSc Thesis* Northeastern University (in Chinese)
[25] Wang C S and Otani Y 2013 *Ind. Eng. Chem. Res.* **52** 5
[26] Nielsen K A and Hill J C 1980 *AIChE J.* **26** 678